DOI: 10.1002/chem.200700046

Diboryl and diboranyl porphyrin complexes Synthesis, structural motifs and chemical reactivity Diborenyl porphyrin or diboranyl isophlorin?

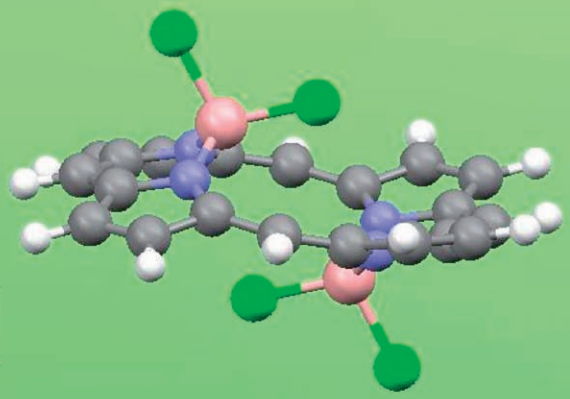

diboryl porphyrin 18 π electrons

-2Cl⁻ +2e⁻

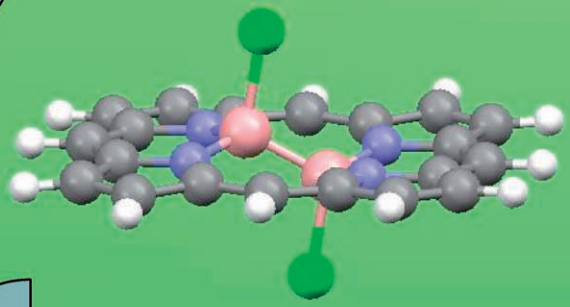

diboranyl porphyrin 18 π electrons

-2Cl⁻ +2e⁻

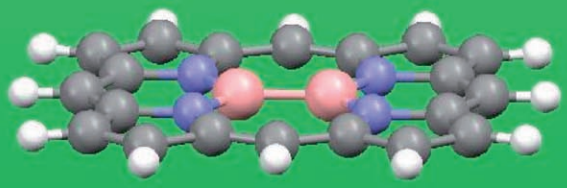

diboranyl isophlorin 20 π electrons

Diboryl and Diboranyl Porphyrin Complexes: Synthesis, Structural Motifs, and Redox Chemistry: Diborenyl Porphyrin or Diboranyl Isophlorin?

Andre Weiss,[a, b] Michael C. Hodgson,[b] Peter D. W. Boyd,[b] Walter Siebert,*[a] and Penelope J. Brothers*[b]

Dedicated to Professor Hubert Schmidbaur

Abstract: The syntheses of diboryl porphyrin complexes $[(BX_2)_2(ttp)]$ (ttp: dianion of tetra-*p*-tolylporphyrin) and the B–B single-bond diboranyl complexes $[(BX)_2(ttp)]$ (X = F, Cl, Br, I) are given. The former are prepared from the reactions of BX_3 (X = F, Cl) with $[Li_2(ttp)]$ and the latter from B_2Cl_4 (X = Cl), the reaction of SbF_3 with $[(BCl)_2(ttp)]$ (for X = F), and, in the cases of X = Br or I, in a remarkable reductive coupling reaction resulting directly from the reaction of BBr_3 or BI_3 with $[Li_2(ttp)]$. Density functional theory (DFT) calculations on the thermochemical parameters for the reductive coupling reactions (and those calculated for related dipyrromethene complexes) indicate that a combination of the reducing ability of bromide and iodide ions combined with the constrained environment of the porphyrin ligand contribute to the driving force. The reductive coupling is also observed in the reaction of $[(BCl_2)_2(ttp)]$ with *n*BuLi to give $[(B\textit{n}Bu)_2(ttp)]$, which was characterised crystallographically. The reaction of $[(BCl)_2(ttp)]$ with catechol gives a boron catecholato porphyrin complex, $[B_2(O_2C_6H_4)(ttp)]$. Chloride abstraction from $[(BCl)_2(ttp)]$ gives the planar dication $[B_2(ttp)]^{2+}$, whereas chemical reduction of $[(BCl)_2(ttp)]$ by using magnesium anthracenide gives a neutral complex, $[B_2(ttp)]$, in which the TTP ligand has been reduced by two electrons to give an unusual example of an isophlorin complex. The cationic and neutral complexes $[B_2(ttp)]^{2+}$ and $[B_2(ttp)]$ were characterised through a combination of spectroscopic data that is supported by DFT calculations on the porphine analogues.

Keywords: boron · density functional calculations · isophlorin · porphyrinoids · redox chemistry

Introduction

The chemistry of main group porphyrin complexes has evolved later than that of the biologically relevant transition-metal porphyrins, but in recent years there has been renewed interest and new results in this area.[1–3] One of our own contributions to this area has been the establishment of the first fully characterised boron–porphyrin complexes, with examples of several different geometries and structural types.[4–7] Interest in boron–porphyrin chemistry derives from intrinsic factors, in particular, the novelty of a porphyrin that contains two central coordinated elements rather than the more usual single atom; the size mismatch between the small boron atom and the coordination site in the macrocycle; and the incompatibility of the usual square-planar, square-pyramidal or octahedral geometry of conventional porphyrin complexes with the tetrahedral or trigonal geometry adopted by boron compounds.

Particular features of boron–porphyrin complexes include, firstly, the coordination of two boron atoms per porphyrin, in which each boron atom is bonded to two adjacent nitrogen atoms. Secondly, a marked tetragonal elongation of the porphyrin ligand is observed, as measured by the nonbonded N···N distance that is parallel to the B···B axis, which is 0.8–1.2 Å longer than the perpendicular N···N distance.[3] In a series of communications we have reported three key structural types for which X-ray crystal structures

[a] Dr. A. Weiss, Prof. Dr. W. Siebert
Anorganisch-Chemisches Institut, Universität Heidelberg
Im Neuenheimer Feld 276, 69121 Heidelberg (Germany)
Fax: (49) 6621-545609
E-mail: walter.siebert@urz.uni-heidelberg.de

[b] Dr. A. Weiss, Dr. M. C. Hodgson, Prof. P. D. W. Boyd, Prof. P. J. Brothers
Department of Chemistry, The University of Auckland
Private Bag 92019, Auckland (New Zealand)
Fax: (+64) 9373-7422
E-mail: p.brothers@auckland.ac.nz

have been obtained. The first is $[B_2OF_2(por)]$ (**1**, Por: unspecified porphyrin dianion), which contains an F–B–O–B–F chain threaded through the centre of the porphyrin,[4,7] and the second is $[B_2O_2(BCl_3)_2(por)]$ (**2**) in which a four-membered B_2O_2 ring is coordinated in the porphyrin cavity perpendicular to the porphyrin plane.[5] A *n*Bu–B–B–*n*Bu singly bonded diborane(6) appears in the third type, $[(BnBu)_2(por)]$ (**3**).[6] A fourth structural type, identified spectroscopically, but not yet crystallographically, is represented by the diboryl complex $[(BCl_2)_2(por)]$ (**4**).[6] Butyl complex **3** can be prepared either by substitution of the chloro ligands in $[(BCl)_2(por)]$ (**5**) by using *n*BuLi (precursor **5** is synthesised from $[Li_2(por)]$ with B_2Cl_4) or directly from the reaction of **4** with *n*BuLi in an unusual and unexpected reductive coupling reaction.[6]

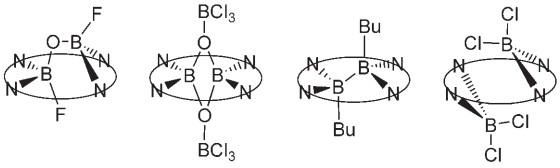

1 2 3 4

In this paper we present experimental details for the formation of the B–B single-bond porphyrin complexes **3** and **5**, diboryl complex **4** and significant new results. These comprise reactions of free-base and lithiated porphyrins with all four boron halides BF_3, BCl_3, BBr_3 and BI_3; further examples of the unexpected reductive coupling reactions to produce $[(BBr)_2(por)]$ and $[(BI)_2(por)]$; and preparation of two new complexes $[B_2(por)]^{2+}$ and $[B_2(por)]$ by ionisation and reduction, respectively, of **5**. The two new species $[B_2(por)]^{2+}$ and $[B_2(por)]$ are the first examples of porphyrin complexes to contain three-coordinate, trigonal-planar boron. The neutral complex $[B_2(por)]$, formally boron(I), offers the intriguing possibility that it may contain a diborene (–B=B–) moiety. However, spectroscopic and density functional theory (DFT) computational evidence indicates that a more appropriate description is a diborane(4) isophlorin.

Results and Discussion

Reactions of H_2(por) and $[Li_2(por)]$ with boron fluorides and chlorides: Our early work focussed on the reaction of the simple boron halides $BF_3{\cdot}OEt_2$ and $BCl_3{\cdot}MeCN$ with free-base porphyrins H_2(ttp) (ttp: dianion of tetra-*p*-tolylporphyrin), H_2(t*p*Clpp) (t*p*Clpp: dianion of 5,10,15,20-tetra-*p*-chlorophenylporphyrin) and H_2(oep) (oep: dianion of 2,3,7,8,12,13,17,18-octaethylporphyrin) in the presence of trace amounts of water, which results in complexes that contain B–O bonds in which the boron–halogen bonds had been partially ($BF_3{\cdot}OEt_2$) or completely ($BCl_3{\cdot}MeCN$) hydrolysed. In the former case, the product was **1**[4,7] and in the latter, the product was **2**,[5] which precipitated from the reaction mixture and was only stable in solution in the presence of excess boron halide. Chromatography of **2** on basic alumina produced $[B_2O(OH)_2(por)]$, which was the hydroxy-substituted analogue of **1**. The formation of **1** or **2** is likely to proceed through hydrolysis of initially formed products of the reactions of boron halides with porphyrin molecules that do not contain oxygen.

To demonstrate this hypothesis, the reaction of BCl_3 with dilithium tetra-*p*-tolylporphyrin $[Li_2(ttp)]$[8] in hexane under strictly anhydrous conditions was undertaken. The green, moisture-sensitive product, $[(BCl_2)_2(ttp)]$ (**4a**), precipitated from the reaction mixture and could be isolated by filtration. Compound **4a** can also be produced from the reaction of the free-base porphyrin $H_2(ttp)$ with BCl_3 in pentane, but the reaction with $[Li_2(ttp)]$ gives a superior yield. The ^{11}B NMR spectrum of the product shows a single resonance at $\delta = 5.6$ ppm, and the ^1H NMR spectrum shows two singlets (1:1 ratio) for the four tolyl methyl groups and a distinctive AB quartet pattern for the H_β protons of the pyrrole rings, which is consistent with C_{2h} or C_{2v} symmetry in the product. The most probable geometry is a transoid arrangement of two BCl_2 groups displaced above and below the porphyrin ring (C_{2h} symmetry), in which each boron atom is coordinated to two porphyrin nitrogen atoms. This geometry is supported by density functional calculations (B3LYP/6-311G(d,p)) on unsubstituted porphyrin analogue **4**, which showed that this geometry is an energy minimum. The calculated bond lengths and angles are consistent with this formulation (Figure 1a). The reaction of **4a** with H_2O (2 equiv) resulted in hydrolysis to form equimolar amounts of $[B_2O_2(BCl_3)_2(ttp)]$ (**2a**) and the porphyrin salt $[H_4(ttp)]Cl_2$, which were both identified by ^1H NMR spectroscopy, and indicated that the oxygen-containing boron–porphyrin products produced in the presence of trace amounts of water are most likely to occur from hydrolysis of **4a** formed initially.

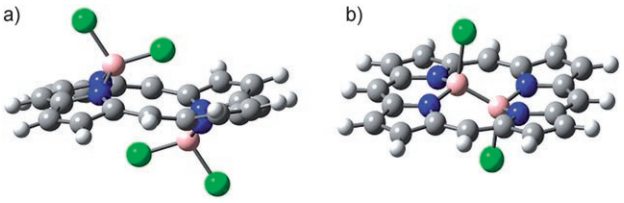

Figure 1. Calculated structures of a) compound **4** and b) compound **5** (B3LYP/6-311G(d,p)).

The cross-ring, non-bonded B···B distance in $[B_2O_2(BCl_3)_2(tpClpp)]$ (**2b**) is 2.05 Å,[5] which indicates that the tetragonal in-plane elongation of the porphyrin macrocycle should readily accommodate a B–B single bond ($r_{cov}(B) = 0.85$ Å[9]). To investigate this possibility, the reaction of B_2Cl_4[10,11] with either $[Li_2(ttp)]$ or $H_2(ttp)$ in hexane at −100 °C gave the product $[(BCl)_2(ttp)]$ (**5a**) in which the B–B single bond present in the B_2Cl_4 precursor is retained.[6]

The reaction containing $[Li_2(ttp)]$ involves elimination of LiCl, whereas in the reaction with $H_2(ttp)$ (or with H_2-(t*p*Clpp) to give **5b**) the free-base porphyrin itself acts as the base, which gives equimolar quantities of **5a** and the doubly protonated porphyrin $[H_4(ttp)]^{2+}$ as the products. The $[H_4(ttp)]Cl_2$ salt precipitates from the non-polar reaction medium, whereas the diboranyl porphyrin remains in solution and allows separation of the products by filtration.

The ^{11}B NMR spectrum of **5a** shows a single resonance at $\delta = -12$ ppm, and the ^1H NMR spectrum is indicative of C_{2h} or C_{2v} symmetry with two singlets for the tolyl methyl groups and a multiplet for the H_β protons of the pyrrole rings. A transoid arrangement (C_{2h} symmetry) of the Cl–B–B–Cl moiety in which the two boron atoms are displaced slightly above and below the porphyrin ring (Figure 1b) is consistent with the ^1H NMR spectroscopy data obtained and is also an energy minimum calculated for **5** (B3LYP/6-311G(d,p)). The B–B distance calculated for **5** is 1.74 Å, which is typical for a B–B single bond.[9]

Views of the computed structures of **4** and **5** are given in Figure 1, and bond lengths and angles in Table 1. It is interesting to compare the extent of the tetragonal porphyrin elongation Δ(N···N) (measured by the difference between the N···N distances parallel and perpendicular to the B–B axis) computed for **4** and **5**, which have values of 1.27 and 0.84 Å, respectively. The porphyrin elongates to a greater extent to accommodate the two bulkier BCl_2 groups in **4**, whereas the much more compact Cl–B–B–Cl moiety in **5** requires less distortion of the macrocycle. The porphyrin in **4** also shows a considerable out-of-plane distortion, which is apparent from the view of the molecule in Figure 1a.

The reaction of $BF_3{\cdot}OEt_2$ with $[Li_2T(ttp)]$ in toluene gave the diboryl product $[(BF_2)_2(ttp)]$ (**6a**). The diboranyl complex $[(BF)_2(ttp)]$ (**7a**) is prepared by substitution of the chlorine atoms in **5a** by using SbF_3 as the fluorinating agent. The two sets of compounds $[(BX_2)_2(ttp)]$ (X = Cl (**4a**), F (**6a**)) and $[(BX)_2(ttp)]$ (X = Cl (**5a**), F (**7a**)) have the same symmetry (C_{2h}), but can be distinguished from each other, in addition to chemical shift differences, by the coupling patterns for the resonance observed for the eight H_β pyrrole protons in their ^1H NMR spectra. The diboryl complexes **4a** and **6a** show a distinct AB quartet for H_β, which appear as two clearly separated doublets or multiplets that each correspond to four protons upon integration. On the other hand, the H_β resonances in the diboranyl compounds **5a** and **7a** appear as one multiplet that corresponds to eight protons upon integration. In each case, the B–B bonded compound (**5a** and **7a**) shows a more upfield chemical shift in the ^{11}B NMR spectrum than the compound with no B–B bond (**4a** and **6a**) does.

Unexpected reductive coupling—Reaction of H_2Por and Li_2Por with boron tribromide and boron triiodide: The reaction of either $H_2(ttp)$ or $[Li_2(ttp)]$ with BBr_3 was carried out with the intention of preparing the bromo analogues of **4a**, **6a**, and $[(BBr_2)_2(ttp)]$ (**8a**). However, the reaction produced a mixture of two compounds that were identified by two sets of resonances in the ^1H NMR spectrum. The most notable feature was that the H_β resonances of the two compounds took two forms, one with an AB quartet similar to that observed for **4a** and **6a**, whereas the second exhibited a multiplet of the form seen for **5a** and **7a**. This result indicated that both compounds **8a** and $[(BBr)_2(ttp)]$ (**9a**) are formed in the reaction of BBr_3 with either $H_2(ttp)$ or $[Li_2T(ttp)]$. An apparently spontaneous reductive coupling of two BBr_2 groups, which formally contain boron(III), occurred to produce the Br–B–B–Br moiety and formed a B–B single bond between two boron(II) centres. The reductant in this system is bromide, although detection of the Br_2 oxidation product proved to be difficult. The proportions of **8a** and **9a** that are formed vary with reaction conditions, but **8a** is the major product. For example, in a typical reaction of $[Li_2(ttp)]$ with BBr_3, the ratio of **8a**:**9a** observed by ^1H NMR spectroscopy is approximately 3:1.

In contrast, the corresponding reaction of $[Li_2(ttp)]$ with BI_3 gives only the dehalogenated product $[(BI)_2(ttp)]$ (**11a**), with no $[(BI_2)_2(ttp)]$ (**10a**) observed at all. Compound **11a** could be isolated and characterised fully, in contrast to **9a** which was always formed in the presence of **8a.** The exclusive formation of the reductively coupled product in the re-

Table 1. Calculated structural parameters for $[(BX_2)_2(porphine)]$ and $[(BX)_2(porphine)]$ (B3LYP/6-311G(d,p)).

	24-atom plane[a] [Å]	Mean N_4 plane[a] [Å]	N···N [Å][b]	ΔN···N [Å][c]	B–X [Å]	B–N [Å]	B–B [Å]	X-B-X [°]	X-B-B [°]
$[(BX_2)_2(porphine)]$									
6 (X = F)	1.189	0.912	3.615, 2.468	1.15	1.367, 1.396	1.580		110.3	
4 (X = Cl)	1.338	0.950	3.725, 2.443	1.28	1.824, 1.926	1.563		104.8	
8 (X = Br)	1.351	0.946	3.732, 2.440	1.29	1.997, 2.138	1.556		102.2	
10 (X = I)	1.331	0.922	3.734, 2.431	1.30	2.224, 2.505	1.538		99.02	
$[(BX)_2(porphine)]$									
7 (X = F)	0.443	0.401	3.317, 2.496	0.82	1.427	1.586	1.727		113.8
5 (X = Cl)	0.393	0.353	3.316, 2.480	0.84	1.957	1.554	1.730		108.6
9 (X = Br)	0.365	0.327	3.319, 2.476	0.84	2.169	1.543	1.724		106.5
11 (X = I)	0.291	0.261	3.326, 2.466	0.86	2.252	1.520	1.707		102.0
3 (X = *n*Bu)	0.495	0.432	3.314, 2.494	0.82	1.640	1.581	1.794		110.3
3a $[(BnBu)_2(ttp)]$[d]	0.499	0.437	3.284, 2.495	0.79	1.611	1.589	1.764		112.9

[a] Displacement from B. [b] Non-bonded N···N distances parallel and perpendicular to the B–B axis. [c] Difference between N···N(parallel) and N···N(perpendicular). [d] Data from X-ray crystal structure.[6]

action with BI_3 is consistent with the stronger reducing power of iodide relative to the lighter halides.

Synthetic routes for the preparation of $[(BX_2)_2(ttp)]$ (**4a**, **6a** and **8a**) and $[(BX)_2(ttp)]$ (**5a**, **7a**, **9a** and **11a**) are summarised in Scheme 1.

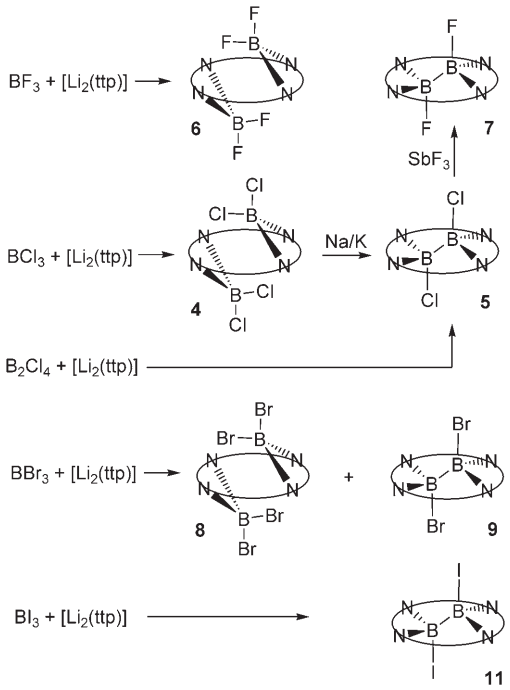

Scheme 1. Synthetic routes for the preparation of $[(BX_2)_2(ttp)]$ (X = F (**6a**), Cl (**4a**), Br (**8a**)) and $[(BX)_2(ttp)]$ (X = F (**7a**), Cl (**5a**), Br (**9a**), I (**11a**)).

DFT calculations of the optimised molecular structure of chloro complex **4** showed that the complex has the largest Δ(N···N) in-plane tetragonal distortion of any of the diboron–porphyrins prepared to date (Table 1). In addition, the calculated structure of **4** showed a marked out-of-plane distortion of the macrocycle (Figure 1a), which indicates that there is considerable crowding in the molecule in order for the porphyrin to accommodate the two bulky BCl_2 groups with tetrahedral geometry at boron. This steric effect should increase in the bromo and iodo analogues. Corresponding structural data have been calculated for the series of complexes $[(BX_2)_2(por)]$ (X = F (**6**), Cl (**4**), Br (**8**) and I (**10**)) and selected structural parameters are given in Table 1. These data show that on going from F to Cl the porphyrin becomes more distorted, which is evident from Δ(N···N) and the displacement of boron from both the mean N_4 and 24-atom planes, but for the Br and I complexes the distortion is no more marked. However, on going down the series of all four halides there is a significant change in the X-B-X angle, which becomes progressively smaller and the outer B–X bond becomes markedly longer than the other. This distortion is evident in Figure 2, which shows a superposition of the calculated molecular structures of (**6**) and $[(BI_2)_2$-(porphine)] (**10**).

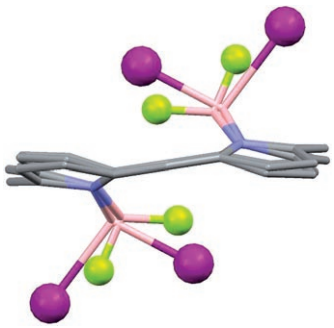

Figure 2. Superposition of structures calculated for $[(BF_2)$(porphine)] (**6**) and $[(BI_2)$(porphine)] (**10**) (B3LYP/6-311G(d,p)). Hydrogen atoms omitted for clarity

The driving force for the spontaneous reductive dehalogenation and B–B bond formation to give **9** and **10** is likely to derive from a combination of the forced close proximity of the two boron atoms within the sterically constrained macrocycle, and the presence of bromide and iodide ions that are able to act as reductants. This hypothesis was examined by thermochemical calculations performed for the coupling reaction shown in Scheme 2a for X = F, Cl, Br or I. The results, given in Table 2, clearly show that for X = Br and I, the reaction is both exothermic and spontaneous in the gas phase, whereas the opposite is true for X = F and Cl, which is in agreement with experimental observations. Whereas this calculation is consistent with the spontaneous reduction reactions, the question of whether or not steric congestion provides the driving force for the reaction was tested by performing similar calculations for the same reaction with the corresponding boryl dipyrromethene (dpm) complexes (Figure 3). These complexes, exemplified by the fluores-

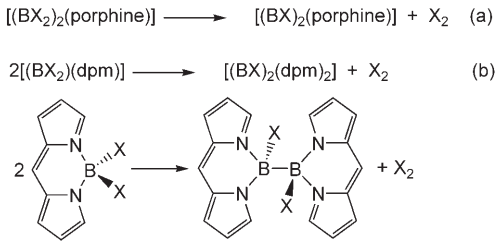

Scheme 2. Reductive coupling reactions for a) porphyrin and b) dipyrromethene (dpm) complexes.

Table 2. Thermochemical calculations for $[(BX_2)_2(por)] \rightarrow [(BX)_2(por)]$ and $2[(BX_2)(dpm)] \rightarrow [(BX)_2(dpm)_2]$.[a]

X	$[(BX_2)_2(por)] \rightarrow [(BX)_2(por)]$		$2[(BX_2)(dpm)] \rightarrow [(BX)_2(dpm)_2]$	
	ΔH [kJ mol^{-1}]	ΔG [kJ mol^{-1}]	ΔH [kJ mol^{-1}]	ΔG [kJ mol^{-1}]
F	715.8	667.4	815.7	862.7
Cl	95.9	46.7	375.8	395.6
Br	−70.9	−119.4	249.4	267.1
I	−212.9	−261.3	168.6	184.8

[a] Optimised structures B3LYP/6-311G(d,p); frequency calculation with unscaled ZPE corrections.

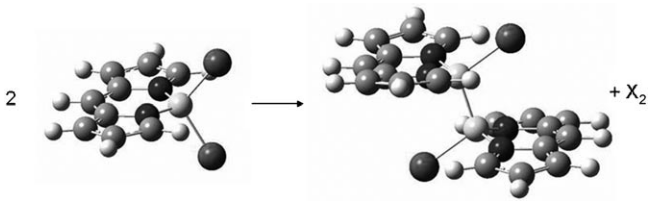

Figure 3. Structures calculated for boryl and diboranyl dipyrromethene (dpm) complexes (B3LYP/6-311G(d,p)).

cence dye BODIPY (4,4-difluoro-4-bora-3a,4a-diaza-*s*-indacene) in which X = F,[12,13] are well known. A [(BX_2)(dpm)] complex can be considered to be a model for half of a [$(BX_2)_2$(por)] complex. The corresponding reaction for which the second set of thermochemical calculations were carried out is shown in Scheme 2b. For the dipyrromethene series, the reductive elimination reaction was not favoured for any halogen, which supports the hypothesis that steric crowding in the porphyrin species contributes to the driving force.

The spontaneous reductive coupling and B–B bond formation to form [$(BX)_2$(ttp)] (X = Br (**9**), I (**10**)) is observed only in the reactions of BBr_3 and BI_3 with [Li_2(ttp)], whereas BCl_3 gives the expected product, **4a**. However, chemical reduction of **4a** by using sodium/potassium alloy as the reductant at −78 °C in toluene effected reductive dehalogenation to produce **5a**, and provides an alternative synthesis of **5a** that does not rely on the use of B_2Cl_4 as the precursor (Scheme 1). Similarly, because the reaction of BI_3 with [Li_2-(ttp)] gives only the B–B bonded product **11a**, this also provides a clean and convenient route to the diboranyl-containing porphyrin that does not require the use of B_2Cl_4.

^{11}B NMR data were collected for the series [$(BX)_2$(ttp)] for X = Cl, Br and I. It is difficult to compare the chemical shifts in the ^{11}B NMR spectrum for the diboranyl porphyrin species because the ^{11}B NMR chemical shifts for the simple boron halides do not vary monotonically down the group owing to the heavy-atom effect.[14] ^{11}B NMR chemical shifts have been calculated (DFT) for the model [$(BX)_2$-(porphine)] complexes described above and are compared with the experimental values observed for [$(BX)_2$(ttp)] (**5a**, **9a** and **11a**) in Table 3.

Reaction of 5a with catechol: The chlorine atoms in the diboryl and diboranyl porphyrin **5a** can be substituted by catechol to give a catecholate complex as the product that demonstrates a new geometry for boron–porphyrins. The reaction of **5a** with catechol in the presence of free-base porphyrin (1 equiv; to act as a base for the catechol protons) in toluene at −78 °C produces a compound identified as [B_2-(cat)(ttp)] (**12a**, cat: dianion of 1,2-$C_6H_4O_2$). The relative intensities of the peaks in the ^{1}H NMR spectrum indicate that only one catecholate ligand is present and the resonances are observed at $\delta = 4.1$ (H_3, H_6) and 5.3 ppm (H_4, H_5). The coordination of catechol to the boron centres was confirmed by the observation of significantly upfield-shifted resonances for the aromatic protons in the catecholate ligand, which is induced by the porphyrin diamagnetic ring current. On the basis of the presence of one catecholate ligand per porphyrin and the symmetry of the overall porphyrin complex observed by ^{1}H NMR spectroscopy, **12a** is proposed to retain the B–B single bond and to contain the B_2(cat) moiety on one face of the porphyrin, with both boron atoms displaced to the same side of the N_4 plane (Scheme 3, Figure 4). Further evidence for the formulation of **12a** comes from the observation of the molecular ion peak by fast atom bombardment mass spectrometry (FABMS).

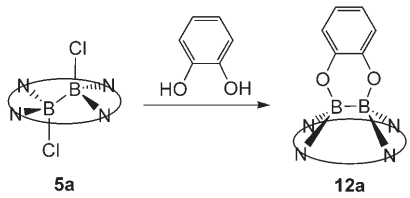

Scheme 3. Reaction of [$(BCl)_2$(ttp)] (**5a**) with catechol to form [B_2(cat)-(ttp)] (**12a**).

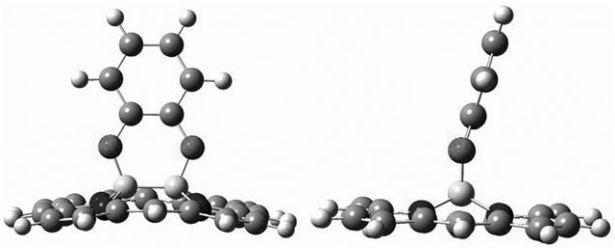

Figure 4. Structure calculated for [B_2(cat)(porphine)] (**12**, cat: 1,2-$C_6H_4O_2$) (B3LYP/6-311G(d,p)).

A DFT calculation of the molecular structure of model complex **12**, Figure 4, gave a minimum energy structure in which the plane of the catecholate moiety is tilted (15°) by folding with respect to the O···O vector from the normal to the porphyrin 24-atom mean plane. The B atoms are 0.82 Å out of the porphyrin plane. However, the higher symmetry, C_{2v}, arrangement in which the catecholate ($C_6H_4O_2$) plane orthogonal to the mean porphyrin plane is < 0.1 kcal mol^{-1} higher in energy. There is a small imaginary frequency that corresponds to the movement of the catecholate between the two possible tilted arrangements indicating that at room temperature an average structure would be observed in the NMR spectrum.

Table 3. Experimental and calculated ^{11}B NMR chemical shifts for diboryl porphyrin complexes.[a]

	Calculated[b]	Experimental[c]
[$(BF)_2$(por)]	−17.5	–
[$(BCl)_2$(por)]	−19.0	−12 to −14 (br)
[$(BBr)_2$(por)]	−18.6	−17.8
[$(BI)_2$(por)]	−8.4	−13.3

[a] Structures optimised B3LYP/6-311G(d,p). Chemical shifts referenced to those calculated for BF_3·Et_2O. [b] Calculated for Por: porphine by using the relativistic ZORA method, which includes spin-orbit contributions (ADF 2003) BPW91/TZP/ZORA. [c] Por: TTP.

Reactions of 4a and 5a with *n*BuLi—Formation of a butyl-substituted complex and a further example of unexpected reductive coupling: The dichlorodiboranyl complex **5a** is extremely hydrolytically sensitive and formation of a derivative by replacing the chloro substituents was undertaken to provide further evidence for the presence of a B–B single bond. The reaction of **5a** with *n*BuLi (2 equiv) at −78 °C in hexane was successful in producing the di-*n*-butyldiboranyl derivative [(B*n*Bu)$_2$(ttp)] (**3a**). Complex **3a**, which was characterised by spectroscopy and an X-ray crystal structure (see below), could also be produced directly by the reaction of **4a** with *n*BuLi (4 equiv) in hexane at −78 °C (Scheme 4).

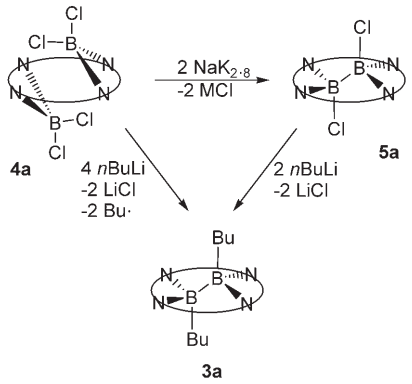

Scheme 4. Reactions of [(BCl$_2$)$_2$(ttp)] (**4a**) and [(BCl)$_2$(ttp)] (**5a**) with *n*BuLi.

This reaction results from both substitution and reduction at the boron centre in precursor **4a**. The expected intermediate is the bis(di-*n*-butyl)boryl complex [(B*n*Bu$_2$)$_2$(ttp)], which may then undergo spontaneous reductive coupling as a result of steric crowding. The fate of the butyl moieties is not clear, and attempts to find suitable trapping reagents for butyl radicals were unsuccessful.

Molecular structure and spectroscopy of 3a: The ^{1}H NMR spectrum of the porphyrin resonances in **3a** indicate that the complex has the same symmetry as precursor **5a**. In addition, the four multiplets that correspond to the butyl resonances are observed, they are well-separated and shifted upfield (ranging from $\delta = -0.56$ for the CH_3 group to -5.70 ppm for the α-CH_2 group) by the diamagnetic porphyrin ring current effect. Similar shifts are observed for the butyl proton resonances in the diamagnetic Group 13 porphyrin complexes [M(*n*Bu)(ttp)] (M = Al,[15] Ga[16] and In[17]), and are compelling evidence for the presence of *n*-butyl groups above and below the porphyrin plane. The structure and ^{1}H and ^{11}B NMR spectra of unsubstituted porphyrin complex **3** have also been calculated (GIAO B3LYP/6-31G(d)//B3LYP/6-311+G(2d,p)), and the upfield chemical shifts calculated for the butyl groups qualitatively match those observed for **3a** in the ^{1}H NMR spectrum (Figure 5). The ^{11}B NMR chemical shift observed for **3a** is $\delta = -6$ ppm and that calculated for **3** is $\delta = -12.5$ ppm.

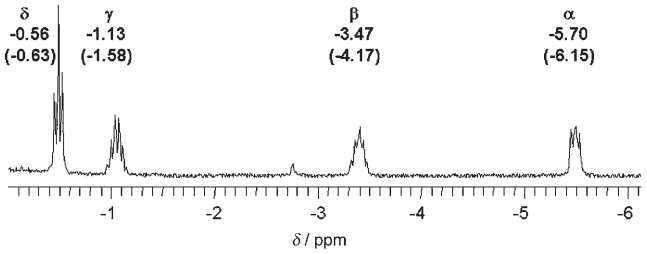

Figure 5. Upfield region of the ^{1}H NMR spectrum of [(B*n*Bu)$_2$(ttp)] **3a** showing experimental and calculated (in brackets) (GIAO B3LYP/6-31G(d)//B3LYP/6-311+G(2d,p)) chemical shifts for the *n*-butyl hydrogen atoms.

The presence of both the butyl substituents and the B–B single bond were confirmed by an X-ray crystal structure determined for a crystal of **3a** grown from dichloromethane.[6] The molecule has an inversion centre, and the two boron atoms are found displaced 0.44 Å above and below the mean N_4 plane. The B–B distance is 1.769(7) Å, which falls within the range for B–B single bonds.[9] The average B–N bond distance, 1.58 Å, is consistent with the sum of the covalent radii of boron (0.89 Å, assumed to be half the B–B bond length in this structure) and sp^2-hybridised nitrogen atom, 0.70 Å.[18] The geometry around the boron atoms is close to tetrahedral, with the six angles around B1 ranging from 104 to 112°. The porphyrin ligand is not completely planar, with the two pyrrole rings bound to B1 tilted up by 6.6 and 8.4°, whereas the other two pyrrole rings are tilted downwards by about the same amount. The porphyrin also shows a marked tetragonal distortion with $\Delta(N\cdots N) = 0.79$ Å. As expected, this is less than the $\Delta(N\cdots N)$ values of 1.09, 1.14, and 1.14 Å observed for the crystal structures of [B$_2$OF$_2$(T*p*Clpp)],[4] [B$_2$OF$_2$(oep)],[7] and [B$_2$O$_2$(BCl$_3$)$_2$-(T*p*Clpp)],[5] in which B–O–B bridges occur. The more compact B–B single-bond moiety requires less elongation of the porphyrin macrocycle. Good agreement is obtained between the structural parameters calculated by using DFT calculations for **3** (Figure 6) and those measured by X-ray crystallography for **3a**.

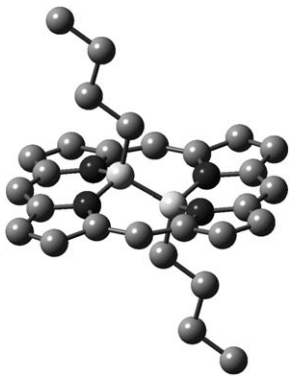

Figure 6. Calculated structure for [(B*n*Bu)$_2$(porphine)] (B3LYP/6-311-G(d)). Hydrogen atoms have been omitted for clarity.

Halogen abstraction from 5a to form the dication $[B_2(por)]^{2+}$: The dication $[B_2(por)]^{2+}$ was prepared by abstraction of the chloride ions from **5a** by treatment with a weakly coordinating anion. Whereas the reactions of **5a** with either $TlPF_6$ in toluene or $NaBPh_4$ in CH_2Cl_2 at ambient temperatures were unsuccessful, the addition of two equivalents of $NaB(Ar_F)_4$ (Ar_F: 3,5-$C_6H_3(CF_3)_2$)[19] in CH_2Cl_2 resulted in the precipitation of NaCl from the reaction medium and the formation of the extremely air- and moisture-sensitive salt $[B_2(ttp)][B(Ar_F)_4]_2$ (**13a**, Scheme 5a).

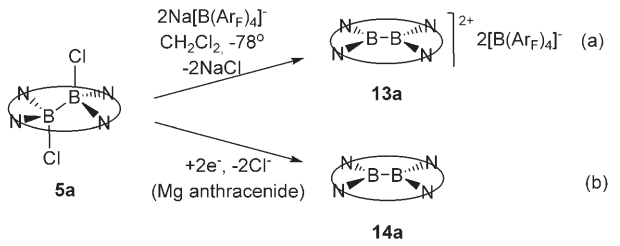

Scheme 5. Preparation of a) $[B_2(ttp)]^{2+}$ (**13a**) and b) $[B_2(ttp)]$ (**14a**).

The complex was characterised by ^{1}H NMR spectroscopy and by observation of the molecular ion peak by means of FABMS. The computed structure (B3LYP/6-311G(d,p)) of the dication $[B_2(porphine)]^{2+}$ (**13**) shows that the complex is planar, in which the two three-coordinate, trigonal-planar boron atoms are in the plane of the porphyrin, and the complex has overall D_{2h} symmetry (Figure 7). The B–B and B–N distances are calculated to be 1.70 and 1.45 Å, which

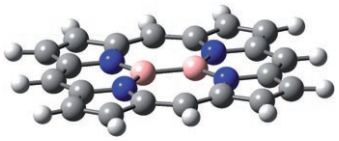

Figure 7. Calculated structure (B3LYP/6-311-G(d,p)) for the cation $[B_2(porphine)]^{2+}$ (**13**).

are both slightly shorter than the corresponding distances (1.73 and 1.557 Å) calculated for precursor **5**. The N-B-N angles in **15** open out to 113° compared with N-B-N angles of 105.6° in **5**. These observations are consistent with the presence of three-coordinate, trigonal-planar boron in **13** versus four-coordinate, tetrahedral boron in **5**.

Chemical reduction of 5a to 14a: The formal two-electron chemical reduction of **4a** by using sodium potassium alloy as the reductant was described above. Compound **4a** contains boron(III), whereas the product, **5a**, contains a B–B single bond and boron(II). The prospect of a further two-electron reduction of **5a** to form a diborene species, which would formally contain boron(I) and a B=B double bond, was intriguing. The chemical reduction of **5a** was achieved by using magnesium anthracenide[20,21] as the reductant in THF at −30 °C. An immediate colour change from green-brown to red-brown was observed, and $MgCl_2$ was formed along with the extremely sensitive black reaction product $[B_2(ttp)]$ (**14a**), which decomposed immediately on contact with air or moisture (Scheme 5b).

The key question concerning the neutral complex **14a** is whether or not it can be described as a diborene, containing boron(I) and a −B=B− moiety coordinated to the porphyrin dianion, or as a diborane(4) in which the diboranyl unit contains boron(II) and the porphyrin ligand has been reduced by two electrons to form the 20-π-electron isophlorin tetraanion. A useful complex for comparison is the cationic diboranyl(4) complex **13a** which formally contains the same boron(II) (B^{II}–B^{II}) moiety, but retains the 18-π-electron porphyrin ligand. Two lines of evidence point towards the formulation of **14a** as a diboranyl(4) isophlorin.

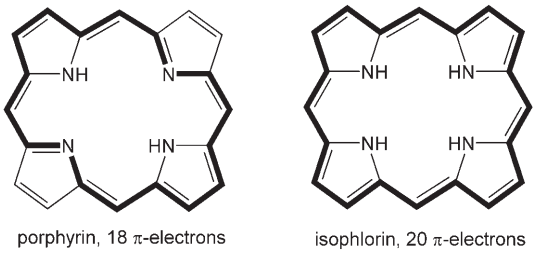

The first line of evidence comes from the ^{1}H NMR spectrum of **14a** in which dramatic chemical shift differences are observed relative to the cationic complex **13a**. These are summarised in Table 4, in which the chemical shifts for **5a** are also given. Both **5a** and **13a** show chemical shifts that are typical for a diamagnetic tetraarylporphyrin complex, in which, for example, the pyrrole H_β protons appear near $\delta =$ 9 ppm. In contrast, the resonances for the H_β protons in **14a** are shifted significantly upfield to $\delta = 0.51$ and 1.05 ppm. The data in Table 4 also show upfield shifts for the other resonances in **14a** relative to those in **5a** and **13a** (H_o, H_m and CH_3). Very similar upfield shifts are observed for the anionic zinc porphyrin species $[Zn(ttp)]^{2-}$ (H_β $\delta = -0.9$ ppm) compared with the neutral complex $[Zn(ttp)]$ (H_β $\delta =$ 9.95 ppm).[22] ^{1}H NMR data for both zinc complexes are also given in Table 4. Two-electron reduction of the neutral complex $[Zn(ttp)]$ results in reduction of the porphyrin macrocycle rather than reduction of the d^{10} zinc(II) metal centre. The ^{1}H NMR chemical shifts observed for $[Zn(ttp)]^{2-}$ have been interpreted as arising from the 20-π-electron, antiaro-

Table 4. Comparison of ^{1}H NMR data for selected boron[a] and zinc[b] porphyrin complexes.

	5a	**13a**	$[Zn(ttp)]$[22]	**14a**	$[Zn(ttp)]^{2-}$[22]
H_β	9.16	9.52	8.95	1.05 0.51	−0.9
H_o	8.22 8.14	8.20	8.10	5.84 5.69	4.95
H_m	7.71 7.62	7.73 7.65	7.55	6.38 6.27	6.05
CH_3	2.76 2.71	2.75 2.70	2.70	1.64 1.62	1.50

[a] $CDCl_3$, 400 MHz. [b] $[D_8]$THF, 400 MHz.

matic isophlorin macrocycle that results from two-electron reduction of the porphyrin ring. More recently, an antiaromatic silicon porphyrin derivative [Si(pyridine)$_2$(tpp)] has been characterised by X-ray structural analysis and NMR spectroscopy.[23] In the solid state the highly ruffled porphyrin shows bond length alternation and in solution there are similar upfield shifts of the pyrrole protons to $\delta = 1.29$ ppm. The similarity of the NMR data for **14a**, $[Zn(tpp)]^{2-}$ and [Si(pyridine)$_2$(tpp)] suggests that a similar conclusion can be drawn for the formulation of **14a** as the diboranyl(4) isophlorin complex.

Further support for the diboranyl(4) isophlorin formulation comes from DFT calculations (B3LYP/6-311G(d,p)) of the molecular structure of [B$_2$(por)] (**14**). The calculated structure shows a planar molecule with the two boron atoms lying in the porphyrin plane, and in that sense is similar to cationic complex **14**. The calculated B–B distance is 1.73 Å, which is similar to the B–B distances calculated for **13** (1.70 Å), **5** (1.737 Å) and **3** (1.790 Å), and observed by X-ray crystallography for **3a** (1.769(7) Å). In particular, the calculated B–B distance is slightly longer for **14** than for **13**, and there is no evidence for the bond shortening that might be observed if a diborene B=B bond was present in **14**. A further feature of the calculated structure of **14** is that the pyrrole rings are differentiated. For example, two diagonally opposite pyrrole rings have shorter C_β–C_β bond lengths (1.35 Å), whereas the other two pyrrole rings have longer C_β–C_β bond lengths (1.40 Å). Overall, **14** has lower symmetry (C_{2h}) than **13** (D_{2h}) for which all the pyrrole rings are equivalent and have, for example, C_β–C_β, bond lengths of 1.369 Å. The calculated alternating bond lengths in the macrocycle in **14** are consistent with the formulation as an isophlorin complex, in which the 20-electron antiaromatic macrocycle has undergone a Jahn–Teller distortion and some alternation of bond lengths is evident. The HOMO calculated by DFT also shows a 20-electron π system (Figure 8).

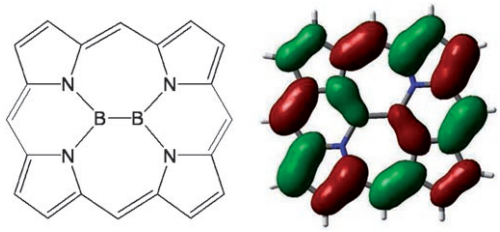

Figure 8. HOMO for [B$_2$(porphine)] (B3LYP/6-311-G(d,p)).

Nucleus-independent chemical shifts (NICS)[24] calculated for **14** and **13** at the centre of the pyrrole rings (NICS(0)) and at a distance of 1 Å above this centre (NICS(1)) clearly indicate a paratropic shift[25] from the aromatic porphyrin dication (NICS(1): $\delta = -16.1$ ppm) to the antiaromatic neutral isophlorin (NICS(1): $\delta = +20.2$ and $+23.4$ ppm). Similar shifts have been calculated in the [Zn(por)] system (NICS(1): $\delta = -9.5$ ppm) and $[Zn(por)]^{2-}$ (NICS(1): $\delta =$ $+23.6$ and $+26.9$ ppm) and in values reported for the [Si(pyridine)$_2$(tpp)] complex.[23] In all three systems the observed pyrrole ^{1}H NMR spectra indicate a rapid interconversion of the single and double bonds with a single signal observed for the zinc and silicon systems and two signals observed for the boron system. A symmetric D_{2h} transition state has been calculated for the interconversion of the two [B$_2$(por)] structures. In the gas phase the enthalpy and free energy of activation have been calculated to be 5.48 and 6.19 kcal mol^{-1}, respectively, which is indicative of a rapid interconversion rate.

The reduction of **13a** to **14a** was also investigated by cyclic voltammetry. Two reversible reduction waves at -1.05 and -1.66 V were observed for **13a** at -30 °C in CH_2Cl_2. The free-base porphyrin (H$_2$(ttp) also undergoes two one-electron reductions under these conditions, at -1.39 and -1.79 V, which indicates that **13a** is more easily reduced than the free-base porphyrin. The opposite situation is observed for the electrochemical reduction of [Zn(ttp)], for which two reversible one-electron reductions were reported at -1.44 and -1.98 V, compared with -1.19 and -1.54 V reported for H$_2$(ttp) under comparable conditions.[22] The higher potential for reduction of the macrocycle in boron complex **13a** relative to [Zn(ttp)] is consistent with the higher net positive charge on dicationic **13a** relative to neutral [Zn(ttp)].

Conclusion

The chemistry of boron–porphyrins has evolved beyond the simple isolation and characterisation of some unusual complexes obtained as a result of the combination of the small element boron with the relatively rigid porphyrin macrocycle. This evolution is marked by the observations, reported in this paper, of unusual chemistry for both the boron and the porphyrin ligand, each occurring as a result of the presence of the other. The remarkable chemistry observed for boron is the spontaneous reductive coupling, first communicated[6] for the reaction of **4a** with *n*BuLi to give the diboranyl species [(B*n*Bu)$_2$(ttp)], and now reported for the reactions of BBr_3 and BI_3 with [Li$_2$(ttp)] to give further diboranyl species **9a** and **11a**. This chemistry does not normally occur with the simple boron halides, and DFT calculations on the thermochemical parameters support the hypothesis that the sterically constrained environment of the porphyrin in the [(BX$_2$)$_2$(ttp)] precursors contributes to the driving force for the reaction.

Unusual chemistry for the porphyrin ligand was observed for the chemical reduction of **5a**, which gave the neutral species **14a**, and was characterised as a complex that contained the 20-electron isophlorin anion. The marked tetragonal elongation of the porphyrin ligand observed in all the boron–porphyrin complexes is another unusual feature of these species, and may give rise to novel electronic and spectroscopic features, which are currently the subject of further investigations.

Finally, the increasing sophistication of DFT calculations has proved invaluable to the work reported here by complementing and in some cases extending the experimental results.

Experimental Section

All syntheses were carried out under an atmosphere of dry argon or nitrogen. Glassware was heated under vacuum and flushed with inert gas prior to use. Solvents were dried according to the usual methods and degassed prior to use. NMR spectra were obtained by using a Bruker DRX 200 spectrometer operating at 200.13 (^{1}H), 64.21 (^{11}B) or 50.32 MHz (^{13}C), an Avance 300 spectrometer operating at 300.13 MHz (^{1}H) or a Bruker DRX 400 spectrometer operating at 400.13 MHz (^{1}H). For ^{1}H and ^{13}C NMR spectroscopy, the residual solvent signals were used as an internal reference, whereas ^{11}B NMR spectra were referenced to the external reference $BF_3{\cdot}OEt_2$. UV/Vis spectra were recorded by using a Perkin–Elmer Lambda 12 spectrometer. Melting points were measured by using a Büchi instrument and are uncorrected. Elemental analyses were determined by using a Heraeus C,H,N,O-Rapid instrument. Mass spectroscopic measurements were made by using a variety of instruments and ionisation methods, which include Varian MAT CH-7 (EI, chemical ionisation (CI)), Jeol JMS 700 (FABMS, low-temperature FABMS (LTFAB)), VG ZAB-2F (EI, high-resolution EI (HREI)), Finnigan TSG 700 (EI, ESI), VG 70-SE (FAB) and HP-5890 II (HP-5971 MSD) (GC–MS(EI)) instruments. Electrochemical measurements were performed by using solutions in dichloromethane that contained 0.1 M [nBu$_4$N][PF$_6$] as the electrolyte, a silver working electrode and a standard Calomel reference electrode. Chemicals were either obtained commercially or were prepared according to literature procedures (H_2(ttp),[26] H_2(TpClpp),[26] [Li_2(ttp)],[27,28] B_2Cl_4,[10,11] magnesium anthracenide,[20,21] Na{[3,5-(CF$_3$)$_2$C$_6$H$_3$]$_4$B} [19]).

[(BnBu)$_2$(ttp)] 3a:[6] nBuLi (2.5 mol L^{-1}; 0.3 mL, 0.75 mmol) was added to a suspension of **5a** (300 mg, 0.35 mmol) in hexane (20 mL) at −78 °C. The reaction mixture was allowed to warm up to RT and was stirred for 16 h. The resulting precipitate was filtered, washed with hexane and extracted with CH_2Cl_2 to yield **3a** as an olive-green solid (200 mg, 71 %). ^{1}H NMR (200 MHz, CD_2Cl_2): δ = 8.34 (AB-q, 8H; H$_\beta$), 7.99 (d, $^3J_{H,H}$ = 8.0 Hz, 4H; H$_{ortho}$), 7.93 (d, $^3J_{H,H}$ = 7.4 Hz, 4H; H$_{ortho}$), 7.58 (d, $^3J_{H,H}$ = 7.9 Hz, 4H; H$_{meta}$), 7.47 (d, $^3J_{H,H}$ = 7.4 Hz, 4H; H$_{meta}$), 2.67 (s, 6H; CH$_3$), 2.63 (s, 6H; CH$_3$), −0.56 (t, $^3J_{H,H}$ = 7.3 Hz, 6H; CH$_3$), −1.13 (m, 4H; γ-CH$_2$), −3.47 (m, 4H; β-CH$_2$), −5.70 ppm (m, 4H; α-CH$_2$); ^{11}B NMR (64.2 MHz, CD_2Cl_2): δ = −6 ppm (br); UV/Vis (CH_2Cl_2): λ_{max} (log ε) = 419 (5.28), 443 (4.92), 517 (4.12), 553 nm (4.00); LTFABMS (toluene): m/z (%): 804 (3) [M]$^+$, 747 (7) [M−C$_4$H$_9$]$^+$, 690 (15) [M−2(C$_4$H$_9$)]$^+$.

[(BCl_2)$_2$(ttp)] 4a: [Li_2(ttp)] (0.28 g, 0.41 mmol) was dissolved in hexane (80 mL) and BCl_3 (1.00 g, 8.53 mmol) was condensed into the reaction mixture at −78 °C. After stirring for 2 h at −78 °C the mixture was allowed to warm to RT and was then stirred for a further 16 h, during which time the product precipitated from the solution. The product was isolated by filtration and washed several times with pentane, extracted into toluene solution and then isolated as a dark blue-violet solid by removal of the toluene under reduced pressure (0.32 g, 95 %). The extremely hydrolytically sensitive product formed green solutions in toluene or halogenated hydrocarbons. Compound **4a** could also be prepared from the reaction of H_2(ttp) (1.58 g, 2.35 mmol) and BCl_3 (1.55 g, 13.2 mmol) in pentane (50 mL) by using a similar procedure (0.36 g, 18 %). M.p. >300 °C; ^{1}H NMR (200 MHz, CD_2Cl_2): δ = 9.45 (br m, 4H; H$_\beta$), 9.11 (br m, 4H; H$_\beta$), 8.45 (d, $^3J_{H,H}$ = 7.9 Hz, 8H; H$_{ortho}$), 7.63 (d, $^3J_{H,H}$ = 7.8 Hz, 8H; H$_{meta}$), 2.74 (s, 6H; CH$_3$), 2.65 ppm (s, 6H; CH$_3$); ^{11}B NMR (64.2 MHz, CD_2Cl_2): δ = 5.6 ppm.

[(BCl)$_2$(ttp)] 5a: A suspension of [Li_2(ttp)] (0.94 g, 1.38 mmol) in hexane (80 mL) was cooled to −100 °C in an ethanol/N_2 (l) bath, and B_2Cl_4 (0.29 g, 1.77 mmol) was condensed into the reaction mixture, which was then stirred for 3 h, then allowed to warm to RT and stirred for a further 12 h. The resulting black powder was collected by filtration, then the product was separated from LiCl by extraction into toluene. After removal of the toluene the product was isolated as a dark-violet powder (0.94 g, 80 %). The solid product contained one equivalent of toluene that could not be removed even under high vacuum. M.p. >300 °C; ^{1}H NMR (200 MHz, CD_2Cl_2): δ = 9.16 (AB-q, 8H; H$_\beta$), 8.22 (d, $^3J_{H,H}$ = 7.9 Hz, 4H; H$_{ortho}$), 8.14 (d, $^3J_{H,H}$ = 7.9 Hz, 4H; H$_{ortho}$), 7.71 (d, $^3J_{H,H}$ = 7.9 Hz, 4H; H$_{meta}$), 7.62 (d, $^3J_{H,H}$ = 7.9 Hz, 4H; H$_{meta}$), 2.76 (s, 6H; CH$_3$), 2.71 ppm (s, 6H; CH$_3$); ^{11}B NMR (64.2 MHz, CD_2Cl_2): δ = −12 ppm (br); UV/Vis (CH_2Cl_2): λ_{max} (log ε) = 370 (3.78), 425 (4.86), 559 (3.60), 605 nm (3.70); LTFABMS (toluene): m/z (%): 760 (1) [M]$^+$, 725 (7) [M−Cl]$^+$, 690 (3) [M−2Cl]$^+$, 671 (4) [M−2B−2Cl+H]$^+$. Compound **5a** was also prepared from the reaction of H_2(ttp) (0.57 g, 0.85 mmol) with B_2Cl_4 (0.16 g, 0.95 mmol) in hexane (20 mL), in a procedure similar to that described for [Li_2(ttp)]. The product was separated from the [H_4(ttp)]Cl_2 residue by extraction with toluene (0.33 g, 92 %).

[(BCl)$_2$(TpClpp)] 5b: The reaction of H_2(TpClpp) (2.16 g, 2.88 mmol) with B_2Cl_4 (0.47 g, 2.88 mmol) in hexane (120 mL) was carried out as described for **5a** to give **5b** (0.95 g, 68 %). ^{1}H NMR (200 MHz, CD_2Cl_2): δ = 9.10 (AB-q, 8H; H$_\beta$), 8.22 (d, $^3J_{H,H}$ = 8.4 Hz, 4H; H$_{ortho}$), 8.14 (d, $^3J_{H,H}$ = 8.1 Hz, 4H; H$_{ortho}$), 7.83 (d, $^3J_{H,H}$ = 8.4 Hz, 4H; H$_{meta}$), 7.74 ppm (d, $^3J_{H,H}$ = 8.2 Hz, 4H; H$_{meta}$); ^{11}B NMR (64.2 MHz, CD_2Cl_2): δ = −14 ppm (br); FABMS (2-nitrophenyl octyl ether (NPOE)): m/z (%): 807 (5) [M−Cl]$^+$, 788 (4) [M−2Cl+O]$^+$, 753 (5) [M−2Cl−2B+2H]$^+$.

[(BF_2)$_2$(ttp)] 6a: [Li_2(ttp)] (0.45 g, 0.66 mmol) was dissolved in toluene (80 mL) and $BF_3{\cdot}OEt_2$ (0.25 g, 1.76 mmol) was added (by syringe) to the reaction mixture at −78 °C. After stirring for 2 h at −78 °C, the mixture was allowed to warm to RT and was then stirred for a further 16 h, during which time the product precipitated from the solution. The insoluble LiF was removed by filtration, and the product was isolated as a mixture of the desired compound together with H_2(ttp) by removal of the toluene from the filtrate under reduced pressure (0.38 g, mixture). M.p. >300 °C; ^{1}H NMR (400 MHz, $CDCl_3$): δ = 8.64 (d, $^3J_{H,H}$ = 4.8 Hz, 4H; H$_\beta$), 8.42 (d, $^3J_{H,H}$ 4.8 Hz, 4H; H$_\beta$), 8.13 (d, $^3J_{H,H}$ = 7.7 Hz, 4H; H$_{ortho}$), 8.10 (d, $^3J_{H,H}$ = 7.5 Hz, 4H; H$_{ortho}$), 7.62 (d, $^3J_{H,H}$ = 7.4 Hz, 8H; H$_{meta}$), 2.76 (s, 6H; CH$_3$), 2.71 ppm (s, 6H; CH$_3$); ^{11}B NMR (64.2 MHz, CD_2Cl_2): δ = −4.0 ppm; FABMS (NBA): m/z (%): 766 (2) [M]$^+$, 744 (7) [M−2F+O]$^+$, 725 (9) [M−3F+O]$^+$; high-resolution FABMS (HRFABMS): calcd for $C_{48}H_{36}{}^{11}B_2F_4N_4$: 766.3062; found: 766.3062.

[(BF)$_2$(ttp)] 7a: Compound **5a** (0.08 g, 0.09 mmol) was dissolved in toluene (15 mL) and SbF_3 (24 equiv) was added. The reaction mixture was stirred at RT for 16 h, filtered, and the deep-violet product **7a** was isolated from the filtrate by removal of the solvent under reduced pressure (0.05 g, 69 %). M.p. >300 °C; ^{1}H NMR (200 MHz, CD_2Cl_2): δ = 9.03 (AB-q, 8H; H$_\beta$), 8.12 (d, $^3J_{H,H}$ = 8.0 Hz, 4H; H$_{ortho}$), 8.07 (d, $^3J_{H,H}$ = 7.9 Hz, 4H; H$_{ortho}$), 7.62 (d, $^3J_{H,H}$ = 7.8 Hz, 4H; H$_{meta}$), 7.54 (d, $^3J_{H,H}$ = 7.8 Hz, 4H; H$_{meta}$), 2.68 (s, 6H; CH$_3$), 2.63 ppm (s, 6H; CH$_3$); ^{11}B NMR (64.2 MHz, CD_2Cl_2): δ = −5.3 ppm; FABMS (NPOE): m/z (%): 744 (10) [M+O]$^+$, 725 (9) [M−F+O]$^+$.

[(BBr_2)$_2$(ttp)] 8a and [(BBr)$_2$(ttp)] 9a: The reaction of [Li_2(ttp)] with BBr_3 was carried out as described for **6a** by using [Li_2(ttp)] (0.29 g, 0.42 mmol) and BBr_3 (0.42 g, 1.66 mmol) in toluene (40 mL) to give a mixture of **8a** and **9a** (0.13 g). Alternatively, the reaction of H_2(ttp) with BBr_3 was carried out as described for **4a** by using H_2(ttp) (0.65 g, 0.97 mmol) and BBr_3 (0.50 g, 2.00 mmol) in hexane (20 mL) to give a mixture of **8a** and **9a** (0.18 g).

*Compound **8a***: ^{1}H NMR (200 MHz, CD_2Cl_2): δ = 9.47 (d, $^3J_{H,H}$ = 4.9 Hz, 4H; H$_\beta$), 9.11 (d, $^3J_{H,H}$ = 4.9 Hz, 4H; H$_\beta$), 8.17 (d, $^3J_{H,H}$ = 7.8 Hz, 8H; H$_{ortho}$), 7.65 (d, $^3J_{H,H}$ = 7.7 Hz, 8H; H$_{meta}$), 2.76 (s, 6H; CH$_3$), 2.65 ppm (s, 6H; CH$_3$); ^{11}B NMR (64.2 MHz, CD_2Cl_2): δ = 15.7 ppm.

*Compound **9a***: ^{1}H NMR (200 MHz, CD_2Cl_2): δ = 9.33 (AB-q, 8H; H$_\beta$), 8.34 (d, $^3J_{H,H}$ = 7.8 Hz, 4H; H$_{ortho}$), 8.28 (d, $^3J_{H,H}$ = 7.9 Hz, 4H; H$_{ortho}$), 7.81 (d, $^3J_{H,H}$ = 7.6 Hz, 4H; H$_{meta}$), 7.73 (d, $^3J_{H,H}$ = 7.6 Hz, 4H; H$_{meta}$), 2.79 (s, 6H; CH$_3$), 2.71 ppm (s, 6H; CH$_3$); ^{11}B NMR (64.2 MHz, CD_2Cl_2): δ = −17.8 ppm.

[(BI)$_2$(ttp)] 11a: The reaction of [Li_2(ttp)] (0.40 g, 0.58 mmol) with BI_3 (0.48 g, 1.23 mmol) in pentane (60 mL) was carried out as described for **4a** (except for the addition of solid BI_3 to the reaction mixture) to give **10a** (0.35 g, 64 %). ^{1}H NMR (200 MHz, $CDCl_3$): δ = 9.61 (AB-q, 8H; H$_\beta$),

8.26 (d, $^3J_{H,H}=7.9$ Hz, 4H; H_{ortho}), 8.19 (d, $^3J_{H,H}=7.9$ Hz, 4H; H_{ortho}), 7.72 (d, $^3J_{H,H}=7.8$ Hz, 4H; H_{meta}), 7.64 (d, $^3J_{H,H}=7.8$ Hz, 4H; H_{meta}), 2.72 (s, 6H; CH_3), 2.66 ppm (s, 6H; CH_3); ^{11}B NMR (64.2 MHz, CD_2Cl_2): $\delta=-13.3$ ppm.

[B_2(cat)(ttp)] 12a: Compound **5a** (0.26 g, 0.31 mmol) and H_2(ttp) (0.21 g, 0.31 mmol) were dissolved in toluene (30 mL) and cooled to −78 °C before the addition of catechol (0.34 g, 0.31 mmol). The mixture was allowed to warm to RT and the insoluble $[H_4(ttp)]Cl_2$ salt was removed by filtration. The solvent was removed from the filtrate to give **12a** as a black solid that was washed with hexane (0.98 mg, 40 %). M.p. >300 °C; ^{1}H NMR (200 MHz, CD_2Cl_2): $\delta=9.10$ (AB-q, 8H; H_β), 8.10 (br d, $^3J_{H,H}=7.9$ Hz, 8H; H_{ortho}), 7.58 (d, $^3J_{H,H}=7.9$ Hz, 4H; H_{meta}), 7.48 (d, $^3J_{H,H}=7.8$ Hz, 4H; H_{meta}), 5.43 (m, 2H; H_{meta}(cat)), 4.15 (m, 2H; H_{ortho}(cat)) 2.69 (s, 6H; CH_3), 2.68 ppm (s, 6H; CH_3); ^{11}B NMR (64.2 MHz, CD_2Cl_2): $\delta=-15$ ppm (br); UV/Vis (CH_2Cl_2): λ_{max} ($\log\varepsilon$)=370 (3.71), 419 (5.12), 516 nm (4.23); FABMS (NPOE): *m/z* (%): 798 (10) $[M]^+$, 690 (18) $[M-C_6H_4O_2]^+$, 671 (40) $[M-C_6H_4O_2B_2+H]^+$.

[B_2(ttp)][$B(Ar_F)_4$]$_2$ 13a: Compound **5a** (0.03 g, 35.1 μmol) was dissolved in CH_2Cl_2 (5 mL) before $Na[B(Ar_F)_4]$ (0.06 g, 67.7 μmol) was added and the solution was stirred for 10 min at RT. NaCl was removed by filtration and the solvent was removed from the filtrate under vacuum to yield **13a** as a green solid (80 mg, 94 %); M.p. >300 °C; ^{1}H NMR (200 MHz, CD_2Cl_2): $\delta=9.52$ (AB-q, 8H; H_β), 8.20 (br m, 8H; H_{ortho}), 7.73 (d, 4H; H_{meta}), 7.65 (d, 4H; H_{meta}), 2.75 (s, 6H; CH_3), 2.70 (s, 6H; CH_3), 7.57 (s, 16H; $H_{ortho}[B(Ar_F)_4]$), 7.36 ppm (s, 8H; $H_{para}[B(Ar_F)_4]$); ^{11}B NMR (64.2 MHz, CD_2Cl_2): $\delta=-6.8$ ppm ($[B(Ar_F)_4]^-$); LTFABMS (toluene): *m/z* (%): 707 (100) $[M+O+H]^+$, 691 (60) $[M+H]^+$, 671 (5) $[M-2B+H]^+$.

[B_2(ttp)] 14a: Compound **5a** (0.24 g, 0.28 mmol) was dissolved in THF (20 mL) and cooled to −30 °C, then $C_{10}H_{14}Mg(THF)_3$ (0.13 g, 1.1 equiv) was added and the mixture was stirred for 30 min. A colour change from brown-green to red-brown was observed. $MgCl_2$ was removed by filtration and the solvent was removed from the filtrate under vacuum. Anthracene was removed from the product by sublimation at 50 °C and 10^{-4} mbar to give **14a** as a black solid. M.p. >300 °C; ^{1}H NMR (200 MHz, CD_2Cl_2): $\delta=6.38$ (d, $^3J_{H,H}=7.6$ Hz, 4H; H_{meta}), 6.27 (d, $^3J_{H,H}=7.6$ Hz, 4H; H_{meta}), 5.84 (d, $^3J_{H,H}=7.6$ Hz, 4H; H_{ortho}), 5.69 (d, $^3J_{H,H}=7.6$ Hz, 4H; H_{ortho}), 2.12 (s, 6H; CH_3), 1.63 (s, 6H; CH_3), 1.05 (d, $^3J_{H,H}=4.4$ Hz, 4H; H_β), 0.51 ppm (d, $^3J_{H,H}=4.4$ Hz, 4H; H_β); ^{11}B NMR (64.2 MHz, CD_2Cl_2): $\delta=-18$ ppm.

Computational details: DFT calculations were carried out by using the Gaussian 03 Program.[29] Full geometry optimisations were carried out for $[(BX_2)_2$(porphine)], $[(BX)_2$(porphine)], $[(BX_2)$(dpm)] (X=F, Cl, Br, I), **12**, **13**, **14** and $[Zn(ttp)]^{2-}$ by using the B3LYP density functional with 6-311G(d,p) basis sets for all elements except for iodine in which a SDD pseudopotential and basis set were used.[30] Harmonic vibrational frequencies were calculated for each structure to verify that each stationary point was a minimum on the molecular hypersurface. These vibrational calculations were used as a basis for the calculation of enthalpies and Gibbs energies in the thermochemical analysis of the reductive elimination reactions of $[(BX_2)_2$(porphine)]. The molecular structure of the $[(BnBu)_2$(porphine)] molecule was optimised by using the B3LYP/6-31G(d) model.

NMR chemical shieldings were calculated by using the GIAO method with the B3LYP/6-311+G(2d,p) model. ^{11}B and ^{1}H NMR spectroscopy chemical shifts were then calculated with reference to chemical shieldings calculated by using the same models for $BF_3{\cdot}(CH_3CH_2)_2O$) and tetramethylsilane, respectively.

For the boron complexes $[(BX)_2$(porphine)] with heavier halogens, ^{11}B NMR spectroscopy chemical shifts were calculated by using the ADF program.[31,32] Calculations were carried out with the BPW91 density functional and TZP, triple zeta all electron basis sets by using the two-component zero-order regular approximation (ZORA) method,[33] which includes spin-orbit coupling. The ADF NMR property module was used to calculate the nuclear shieldings by using the spin-orbit ZORA method with the geometries obtained from above (B3LYP/6-311G(d,p)).[33,34] Calculated chemical shifts were determined by the difference between the shielding in these molecules and those calculated for the reference $BF_3{\cdot}((CH_3CH_2)_2O)$.

Acknowledgements

The authors are grateful to the Marsden Fund (administered by the Royal Society of New Zealand), the University of Auckland Research Committee and the Deutsche Forschungsgemeinschaft (DFG) for financial support.

[1] J. K. M. Sanders, N. Bampos, Z. Clyde-Watson, S. L. Darling, J. C. Hawley, H. J. Kim, C. C. Mak, S. J. Webb in *The Porphyrin Handbook, Vol. 3* (Eds.: K. M. Kadish, K. M. Smith, R. Guilard), Academic Press, San Diego, **1999**, pp. 1.
[2] P. J. Brothers, *Adv. Organomet. Chem.* **2001**, *48*, 289.
[3] P. J. Brothers, *J. Porphyrins Phthalocyanines* **2003**, *6*, 259.
[4] W. J. Belcher, P. D. W. Boyd, P. J. Brothers, M. J. Liddell, C. E. F. Rickard, *J. Am. Chem. Soc.* **1994**, *116*, 8416.
[5] W. J. Belcher, M. Breede, P. J. Brothers, C. E. F. Rickard, *Angew. Chem.* **1998**, *110*, 1133; *Angew. Chem. Int. Ed.* **1998**, *37*, 1112.
[6] a) A. Weiss, H. Pritzkow, P. J. Brothers, W. Siebert, Angew. Chem. 2001, *113*, 4311; *Angew. Chem. Int. Ed.* **2001**, *40*, 4182; b) A. Weiss, PhD thesis, University of Heidelberg (Germany), **2002**.
[7] T. Köhler, M. C. Hodgson, D. Seidel, J. M. Veauthier, S. Meyer, V. Lynch, P. D. W. Boyd, P. J. Brothers, J. L. Sessler, *Chem. Commun.* **2004**, 1060.
[8] J. Arnold, D. Y. Dawson, C. G. Hoffman, *J. Am. Chem. Soc.* **1993**, *115*, 2707.
[9] A. Moezzi, M. M. Olmstead, P. P. Power, *J. Am. Chem. Soc.* **1992**, *114*, 2715.
[10] P. L. Timms, *J. Chem. Soc. Dalton Trans.* **1972**, 830.
[11] H. Schulz, Diplomarbeit, Universität Heidelberg (Germany), **1988**.
[12] E. Vos De Wael, E. J. A. Pardoen, J. A. van Koeveringe, J. Lugtenburg, *Recl. Trav. Chim. Pays-Bas* **1977**, *96*, 306.
[13] J. V. Bonfiglio, R. Bonnett, D. G. Buckley, D. Hamzetash, M. B. Hursthouse, K. M. A. Malik, A. F. McDonagh, J. Trotter, *Tetrahedron* **1983**, *39*, 1865–1874.
[14] Personal communication, P. D. W. Boyd, **2004**.
[15] R. Guilard, A. Zrineh, A. Tabard, A. Endo, B. C. Han, C. Lecomte, M. Souhassou, A. Habbou, M. Ferhat, K. M. Kadish, *Inorg. Chem.* **1990**, *29*, 4476.
[16] K. M. Kadish, B. Boisselier-Cocolios, A. Coutsolelos, P. Mitaine, R. Guilard, *Inorg. Chem.* **1985**, *24*, 4521.
[17] P. Cocolios, R. Guilard, P. Fournari, *J. Organomet. Chem.* **1979**, *179*, 311.
[18] J. E. Huheey, E. A. Keiter, R. L. Keiter, *Inorganic Chemistry*, 4th ed, Harper Collins, New York, **1993**.
[19] D. L. Reger, T. D. Wright, C. A. Little, J. J. S. Lamba, M. D. Smith, *Inorg. Chem.* **2001**, *40*, 3810.
[20] B. Bogdanovic, S. Liao, R. Mynott, K. Schlichte, U. Westeppe, *Chem. Ber.* **1984**, *117*, 1387.
[21] B. Bogdanovic, N. Janke, C. Krüger, R. Mynott, K. Schlichte, U. Westeppe, *Angew. Chem.* **1985**, *97*, 972; *Angew. Chem. Int. Ed. Engl.* **1985**, *24*, 960.
[22] R. Kosmo, C. Kautz, K. Meerholz, J. Heinze, K. Müllen, *Angew. Chem.* **1989**, *101*, 638; *Angew. Chem. Int. Ed. Engl.* **1989**, *28*, 604.
[23] J. A. Cissell, T. P. Vaid, A. L. Rheingold, *J. Am. Chem. Soc.* **2005**, *127*, 12212.
[24] Z. Chen, C. S. Wannere, C. Corminboeuf, R. Puchta, P. von R. Schleyer, *Chem. Rev.* **2005**, *105*, 3842.
[25] J. A. Pople, K. G. Untchl, *J. Am. Chem. Soc.* **1966**, *88*, 4811.
[26] A. D. Adler, F. R. Longo, J. D. Finarelli, J. Goldmacher, J. Assour, L. Korsakoff, *J. Org. Chem.* **1967**, *32*, 476.
[27] J. Arnold, *J. Chem. Soc. Chem. Commun.* **1990**, 976.
[28] H. Brand, J. A. Capriotti, J. Arnold, *Inorg. Chem.* **1994**, *33*, 4334.
[29] Gaussian 03, Revision B.03, M. J. Frisch, G. W. Trucks, H. B. Schlegel, G. E. Scuseria, M. A. Robb, J. R. Cheeseman, J. A. Montgomery, Jr., T. Vreven, K. N. Kudin, J. C. Burant, J. M. Millam, S. S. Iyengar, J. Tomasi, V. Barone, B. Mennucci, M. Cossi, G. Scalmani, N. Rega, G. A. Petersson, H. Nakatsuji, M. Hada, M. Ehara, K. Toyota, R. Fukuda, J. Hasegawa, M. Ishida, T. Nakajima, Y. Honda,

O. Kitao, H. Nakai, M. Klene, X. Li, J. E. Knox, H. P. Hratchian, J. B. Cross, V. Bakken, C. Adamo, J. Jaramillo, R. Gomperts, R. E. Stratmann, O. Yazyev, A. J. Austin, R. Cammi, C. Pomelli, J. W. Ochterski, P. Y. Ayala, K. Morokuma, G. A. Voth, P. Salvador, J. J. Dannenberg, V. G. Zakrzewski, S. Dapprich, A. D. Daniels, M. C. Strain, O. Farkas, D. K. Malick, A. D. Rabuck, K. Raghavachari, J. B. Foresman, J. V. Ortiz, Q. Cui, A. G. Baboul, S. Clifford, J. Cioslowski, B. B. Stefanov, G. Liu, A. Liashenko, P. Piskorz, I. Komaromi, R. L. Martin, D. J. Fox, T. Keith, M. A. Al-Laham, C. Y. Peng, A. Nanayakkara, M. Challacombe, P. M. W. Gill, B. Johnson, W. Chen, M. W. Wong, C. Gonzalez, J. A. Pople, Gaussian, Inc., Wallingford CT, **2004**.

[30] G. Igel-Mann, H. Stoll, H. Preuss, *Mol. Phys.* **1988**, *65*, 1321.

[31] Amsterdam Density Functional (ADF), Release 2003, Theoretical Chemistry, Vrije Universiteit, De Boelelaan 1083, 1081 HV Amsterdam, The Netherlands.

[32] G. te Velde, F. M. Bickelhaupt, E. J. Baerends, C. Fonseca Guerra, S. J. A. van Gisbergen, J. G. Snijders, T. Ziegler, *J. Comput. Chem.* **2001**, *22*, 931.

[33] S. K. Wolff, T. Ziegler, E. van Lenthe, E. J. Baerends, *J. Chem. Phys.* **1999**, *110*, 7689.

[34] E. van Lenthe, E. J. Baerends, J. G. Snijders, *J. Chem. Phys.* **1993**, *99*, 4597.

Received: January 11, 2007
Published online: June 15, 2007

